

Native Celluloses on the Basis of Two Crystalline Phase ($I\alpha/I\beta$) System

MASAHISA WADA,* JUNJI SUGIYAMA, and TAKESHI OKANO

Department of Forest Products, Faculty of Agriculture, The University of Tokyo, Yayoi 1-1-1, Bunkyo-ku, Tokyo 113, Japan

SYNOPSIS

A survey by X-ray diffractometry was carried out to confirm the two crystalline phase $I\alpha/I\beta$ (triclinic/monoclinic) system of native celluloses. We have investigated cellulose samples from 12 different origins and measured the d -spacings with reasonable precision. The samples were then subjected to the hydrothermal annealing that brings the cellulose crystals to the monoclinic type; d -spacings were reevaluated afterward. From the statistical analysis using observed d -spacings, all the cellulose samples were categorized into the two groups that coincide with the two crystalline phase systems: one is the algal-bacterial type rich in triclinic phase and the other is the cotton-ramie type of the monoclinic phase. © 1993 John Wiley & Sons, Inc.

INTRODUCTION

During the last decade the solid state ^{13}C NMR became available for the structural investigation of cellulose crystallites^{1,2} and particularly the CP/MAS technique revealed the spectral differences among variety of cellulose origins.³⁻⁶ Atalla and VanderHart^{3,4} first demonstrated that the multiplicity of the conformationally important carbon atoms (C1, C4, and C6) were different between the algal-bacterial cellulose and the cotton-ramie cellulose. They proposed a two crystalline phase model in that all the native celluloses were the composite of $I\alpha$ and $I\beta$, despite the fact that the exact structures of $I\alpha$ and $I\beta$ were not established. According to this scheme, the algal-bacterial type celluloses are rich in $I\alpha$ component, whereas the cotton-ramie type celluloses are rich in $I\beta$.

After thorough investigation, important features of these two phases has been found:

1. $I\alpha$ transforms into low crystalline $I\beta$ by deswelling from EDA-cellulose $I\alpha$ complex,⁷

and by saponifying CTA prepared from $I\alpha$ cellulose.⁸

2. $I\beta$ type is thermodynamically more stable than $I\alpha$ phase because $I\alpha$ transforms into $I\beta$ after hydrothermal annealing.^{9,10}
3. Pure $I\beta$ exists in the cellulose from tunicin.¹¹
4. $I\alpha$ and $I\beta$ may have a different H-bonding pattern since their FT-IR spectra are not identical in the OH stretching region.¹²
5. From selected area diffraction¹³ and microdiffraction in electron microscopy,¹⁴ $I\alpha$ and $I\beta$ are characterized as crystals consisting of one chain triclinic unit cell and two chain monoclinic unit cell, respectively.¹³

In this article, we examine native celluloses on the basis of this two crystalline phase system by X-ray diffractometry widely used by both physicists and chemists. X-ray diffractometry is more universal in comparison with the sophisticated methods such as solid state ^{13}C NMR and electron diffraction. By using this method, the very small shifts of peak positions for *Valonia* cellulose before and after hydrothermal annealing was pointed out by Yamamoto et al.¹⁰ Therefore we carried out the quantitative statistical analysis on the d -spacing data that are measurable from whole x-ray diffractometry profiles to characterize and classify native celluloses.

* To whom correspondence should be addressed.

EXPERIMENTAL

Materials

In this study we used twelve kinds of celluloses. They were from four origins: sea algae, bacterial products, higher plants (including commercial products), and an animal.

The vesicles of *Valonia aegagropia*, *Valoniopsis pachynema*, and *Boergesenia forbesii*, gifts from Mr. S. Ui, were harvested from the sea at Kuroshima, Okinawa. Whole plants of *Cladophora sp.* were collected in the sea at Chikura, Chiba. A purified sample of *Rhizoclonium sp.* was a gift from Dr. R. Atalla. *Chaetomorpha crassa* were harvested from the tide pool at Suzaki, Shizuoka. A purified mat of *Acetobacter cellulose*, a gift from Rengo Inc., was stored in ethanol. A sample of microcrystalline cellulose was Avicel SF (Asahi Chem. Co.). A commercial cotton linter ACALA SJ-2 was also used. Cactus hairs of *Cephalocereus senilis* and *Pilocereus palmeli* were collected in Okinawa. The test of *Halocynthia sp.* was taken from the sea fruit commercially available.

The celluloses of *Valonia aegagropia*, *Valoniopsis pachynema*, and *Boergesenia forbesii* were purified by boiling in 0.1 N NaOH for 6 h with solvent exchange of every 2 h, followed by immersion overnight in 0.05 N HCl at room temperature. They were then washed in distilled water and stored in water with a few drops of chloroform. The cell walls of *Cladophora sp.* and *Chaetomorpha crassa*, cotton fibers, cactus hairs of *Cephalocereus senilis* and *Pilocereus palmeri*, and the test of *Halocynthia sp.* were purified by bleaching in 0.3% NaClO₂ at 80°C for 4 h, the solution was buffered at pH 4.9 in acetate buffer. This was followed by overnight immersion in 5% KOH and a thorough washing in distilled water. These treatments were repeated until the samples became perfectly white. The samples were then stored in water with a few drops of chloroform.

All samples were disintegrated into small fragments with a double cylinder homogenizer. They were then freeze dried and reformed by pressing into the plate for x-ray measurements (diameter, 6 mm; thickness, 1 mm).

X-Ray Measurements

X-ray measurements were carried out with a transmission method by JEOL JDX5 diffractometer. Ni-filtered Cu-K α radiation ($\lambda = 0.1542$ nm) generated at 35 kV and 25 mA was collimated by a pinhole of 0.6 mm ϕ with a length of 68 mm. The intensities of

diffracted beams from samples, which passed through a pinhole of 0.2 mm ϕ with a length of 147 mm, were measured with a scintillation counter equipped with a pulse height analyzer. The scanning was made through $2\theta = 10\text{--}40^\circ$. Intensity data was recorded with a digital recorder.

Separation of peaks were carried out using a least-squares refinement program¹⁵ in order to avoid the possible errors caused by the subjectivity of operators. In the process, each crystalline peak was assumed to be a Gaussian function [$G(2\theta)$].

$$G(2\theta) = A \exp[-(B - 2\theta)^2/2C^2]$$

where A is peak height, B is mean (Bragg angle), and C is standard deviation. The diffraction angle was calibrated every time with a sodium fluoride diffraction line ($d = 0.2319$ nm).

Hydrothermal Treatment

Each purified sample was inserted into a small glass ampule filled with a small amount of 0.1 N NaOH. The ampule was sealed and inserted in an autoclave to which a small amount of water was also added to build a counter pressure during the annealing. The autoclave was hermetically sealed and heated in an oil bath to 260°C. After maintaining for 30 min, the autoclave was cooled down under tap water. The annealed samples were washed thoroughly by filtering with excess water under reduced pressure. They were then freeze dried and reshaped into a disk for x-ray measurements.

RESULTS

Typical X-ray diffractometry curves are shown in Figure 1. They were obtained from highly crystalline *Halocynthia* (upper) and *Valonia* (lower) celluloses, respectively. In general there were seven crystalline peaks in the 2θ range of 10–40°. Among them, those peaks numbered as 1, 2, 3, 4, and 7 are always clearly identified. The remainders, peaks 5 and 6, however, were not clear in the case of celluloses of lower crystallinity such as Avicel and cotton. We thus focused on the above five peaks for further analysis.

According to the two crystalline phase system, *Valonia* contains both the triclinic and monoclinic component whereas *Halocynthia* cellulose consists of entirely monoclinic component. Thus all the peaks in *Valonia* have to be interpreted in terms of two crystalline structures: the triclinic structure with dimensions of $a = 0.674$ nm, $b = 0.593$ nm, $c = 1.036$

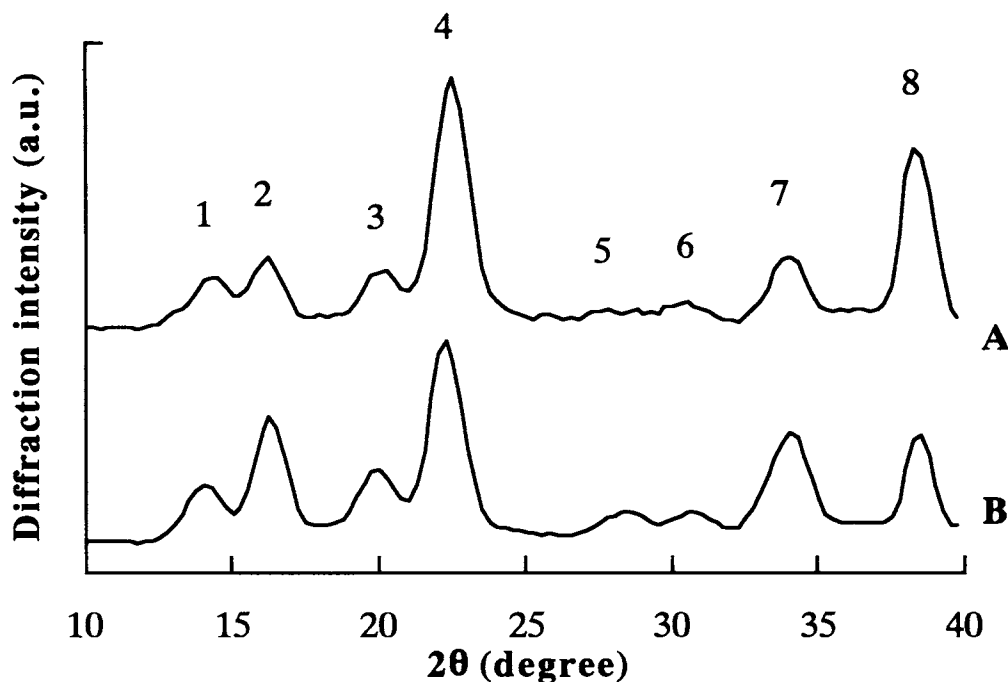


Figure 1 Typical X-ray diffractometry curves of *Halocynthia* cellulose (A) and *Valonia* cellulose (B). Peaks 1–7 derive from cellulose crystals, but peak 8 is the diffraction line of NaF ($2\theta = 38.84^\circ$).

nm, $\alpha = 117^\circ$, $\beta = 113^\circ$, and $\gamma = 81^\circ$; and the monoclinic structure with dimensions of $a = 0.801$ nm, $b = 0.817$ nm, $c = 1.036$ nm, and γ (monoclinic angle) = 97.3° .¹⁴ Because of the superposition of these two structures we recognize that each peak has at least two indices, summarized in Table I. It is also worthwhile to note that the d -spacings calculated from the proposed triclinic and monoclinic structures are slightly different.^{9,14}

For simplicity, let us first consider peak 1, which is a composite of the (100) triclinic and the ($1\bar{1}0$) monoclinic diffractions. As the (100) interplaner spacing is larger than ($1\bar{1}0$), it is natural to obtain larger spacing if the triclinic crystals are dominant. In the opposite case, smaller values should be obtained. Second, peak 2 is the composite of (010) triclinic and the (110) monoclinic diffractions. Be-

cause the (010) triclinic spacing is smaller than (110), the more the triclinic components the smaller d -spacings would result. Those are simply derived from the reported unit cells¹⁴ and should be detected also by X-ray measurements.

The results of observed d -spacings from initial cellulose samples were summarized in Table II. Seven cellulose samples from the top (a–g) belong to the so-called algal-bacterial type that consists of two crystalline moieties $I\alpha$ (triclinic) and $I\beta$ (monoclinic). The rests (h–l) are from the cotton-ramie type that mainly consists of $I\beta$ (monoclinic) component. Apparently the d -spacings of peaks 1 and 2 are different between two groups as predicted from the unit cell dimensions.

Despite the clear difference in d_1 and d_2 , the rest, mainly d_3 and d_4 are not obvious. Particularly, d_4

Table I Interpretation of Major Reflections in Terms of Two Crystalline Phase Model

Peak No.	1	2	3	4	7
Approx. Bragg angle (deg.)	14.5	16.6	20.4	22.7	34.4
Triclinic	(100)	(010)	($\bar{1}\bar{1}2$)	(110)	($\bar{1}\bar{2}3$) ($\bar{1}\bar{1}4$)
Indices and d -spacings (nm)	0.621	0.528	0.438	0.397	0.269 0.259
Monoclinic	($1\bar{1}0$)	(110)	(012) (102)	(200)	(023) (004)
Indices and d -spacings (nm)	0.607	0.535	0.436 0.434	0.397	0.263 0.259

Table II *d*-Spacings of Initial Celluloses

Initial	<i>d</i> -Spacings (nm)				
	<i>d</i> ₁	<i>d</i> ₂	<i>d</i> ₃	<i>d</i> ₄	<i>d</i> ₇
(a) <i>Valonia</i>	0.614	0.531	0.437	0.392	0.261
(b) <i>Valoniopsis</i>	0.609	0.531	0.435	0.392	0.261
(c) <i>Boergesenia</i>	0.610	0.529	0.434	0.391	0.260
(d) <i>Cladophora</i>	0.612	0.530	0.435	0.391	0.260
(e) <i>Rhizoclonium</i>	0.613	0.532	0.435	0.393	0.261
(f) <i>Chaetomorpha</i>	0.613	0.533	0.438	0.392	0.261
(g) Bacterial	0.611	0.531	0.437	0.394	0.260
(h) Avicel	0.607	0.544	0.436	0.395	0.260
(i) Cotton	0.608	0.540	0.435	0.393	0.260
(j) <i>Cephalocereus</i>	0.606	0.535	0.436	0.393	0.260
(k) <i>Pilocereus</i>	0.608	0.536	0.434	0.394	0.260
(l) <i>Halocynthia</i>	0.604	0.534	0.434	0.389	0.261

seems to be influenced by the crystallite size rather than the ratio of I α and I β components. In fact, *d*₄ values are in the order of tunicate < algae < cotton, Avicel, and cactus celluloses; smaller *d*₄ values correspond to the large crystal. Little change has been found in *d*₇, the meridional reflection that can be indexed as ($\bar{1}\bar{1}4$) by the triclinic cell and (004) by the monoclinic cell. This is because fiber repeats of two models are identical.

X-ray diffractometry curves of *Cladophora* cellulose before and after annealing were presented in Figure 2. After hydrothermal treatment peak 1 shifted to wider angles; otherwise, peak 2 shifted to lower angles. These shifts are based on the transformation from the (100) and the (010) triclinic diffraction into the ($\bar{1}\bar{1}0$) and the (110) monoclinic diffraction, respectively. It is also noticeable that peak 4 moved to slightly wider angles. These results are similar to that reported by Yamamoto et al.¹⁰

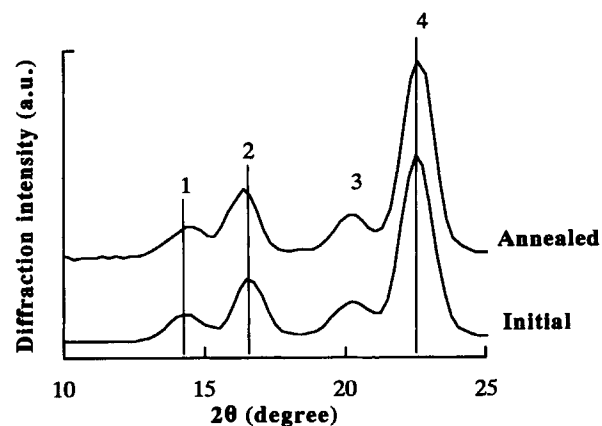


Figure 2 X-ray diffractometry curves of initial and annealed *Cladophora* cellulose.

The *d*-spacings of annealed celluloses are listed in Table III. Clearly the difference between algal-bacterial type (upper 7 specimens) and cotton-ramie type (lower 5 specimens) is diminished. For example, the *d*₁ and *d*₄ became smaller and the *d*₂ increased slightly in comparison with the initial cellulose data in Table II. In particular all the highly crystalline algal celluloses have almost identical features with *Halocynthia* that scarcely shows differences before and after the annealing. The results are in good agreement with the fact that I α cellulose transforms to I β type without losing crystallinity by hydrothermal treatment.^{10,13} The other lower crystalline celluloses such as Avicel, cotton, and cactus hair, however, were partially hydrolyzed and also broken into smaller particles so that the figures in Table III, for instance *d*₂ and *d*₄ are larger than those of the monoclinic celluloses of higher crystallinity (i.e., *Halocynthia* and annealed algal cellulose). The possible reason will be discussed later.

DISCUSSION

The observed *d*-spacing data contains mixed information of both I α and I β structures. Thus, we applied statistical treatment to extract the specific feature from each structure by analyzing all the *d*-spacing data available. For this, we adopted discriminant analysis. We defined two groups in advance. The discriminant function between algal-bacterial type and cotton-ramie type was given by:

$$Z = 1364d_1 - 1325d_2 - 148d_3 + 1578d_4 + 3566d_7 - 1606,$$

Table III *d*-Spacings of Annealed Celluloses

Annealed	<i>d</i> -Spacings (nm)				
	<i>d</i> ₁	<i>d</i> ₂	<i>d</i> ₃	<i>d</i> ₄	<i>d</i> ₇
(a) <i>Valonia</i>	0.604	0.534	0.435	0.387	0.261
(b) <i>Valoniopsis</i>	0.602	0.535	0.434	0.388	0.260
(c) <i>Boergesenia</i>		0.537	0.435	0.389	0.261
(d) <i>Cladophora</i>	0.605	0.533	0.433	0.389	0.261
(e) <i>Rhizoclonium</i>	0.605	0.533	0.433	0.389	0.261
(f) <i>Chaetomorpha</i>	0.604	0.533	0.434	0.388	0.261
(g) Bacterial	0.598	0.532	0.435	0.392	0.260
(h) Avicel				0.437	0.393
(i) Cotton	0.601	0.544	0.432	0.392	0.260
(j) <i>Cephalocereus</i>	0.604	0.541	0.432	0.393	0.259
(k) <i>Pilocereus</i>	0.605	0.545	0.434	0.394	0.260
(l) <i>Halocynthia</i>	0.604	0.533	0.434	0.388	0.261

where $Z > 0$, algal-bacterial type ($I\alpha$ triclinic rich); $Z < 0$, cotton-ramie type ($I\beta$ monoclinic dominated).

In the bottom of Figure 3, a histogram of Z values obtained from d -spacing data of initial celluloses is shown, where algal-bacterial type is clearly different from cotton-ramie type. We then calculated discriminant Z values of annealed specimens and the results are represented in the top of Figure 3. Clearly the discriminant Z values of annealed algal-bacterial type were all minus. This means that the triclinic phase was transformed into the monoclinic phase by annealing, which is consistent with the previous

report of Yamamoto et al.¹⁰ Those data of annealed *Boergesenia* and Avicel cellulose were missing in Figure 3. They are considerably degraded after annealing so that we could not collect d -spacings that are necessary to perform the above analysis. However, we believe this does not alter the above conclusion.

As reported by Debzi et al.,¹⁶ although an alkaline annealing is the most effective way to proceed in the conversion from $I\alpha$ to $I\beta$, there is always some $I\alpha$ left. This minor signal is detectable by ¹³C NMR technique. The other techniques such as FT-IR,¹²

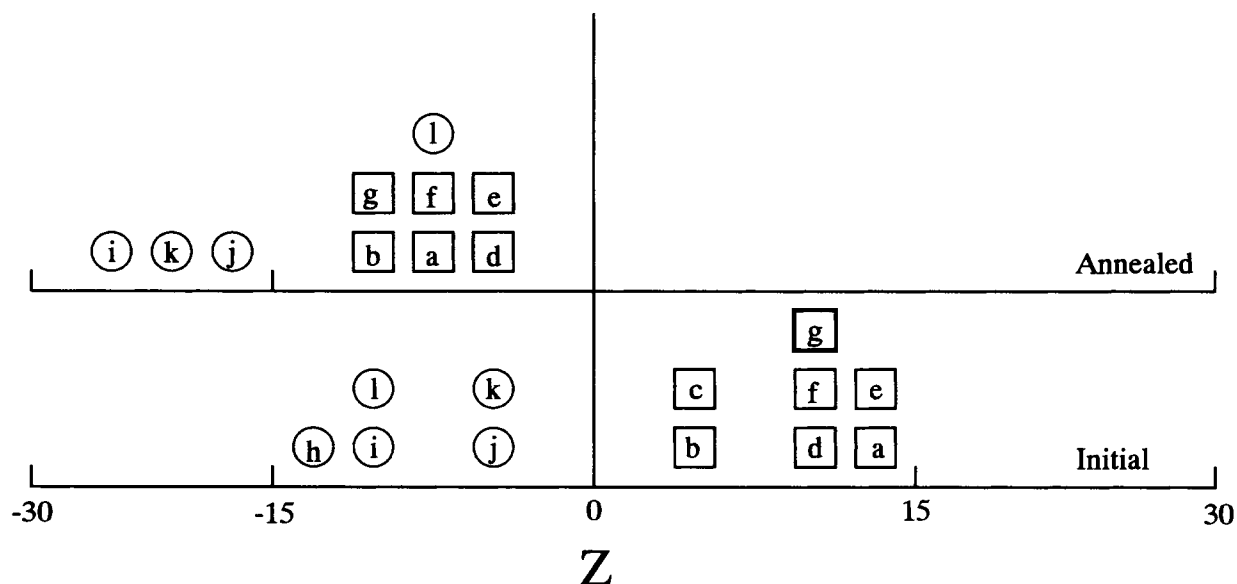


Figure 3 Histograms of the discriminant function Z . (\square) algal-bacterial type; (\circ) cotton-ramie type. (a-l) indicate the corresponding cellulose samples listed in Tables II and III.

electron diffraction,^{13,14} and X-ray diffraction in this study, cannot detect the remaining I α component in the materials. This may be because the ¹³C NMR is uniquely sensitive to such a local structure, and also because I α domain is too small or disordered to generate Bragg reflection.

The discriminant *Z* values of cotton, *Cephalocereus*, and *Pilocereus* shifted also to minus after annealing. The shift was as large as that of the algal-bacterial type. Regarding this change, one may see in the histogram of initial celluloses that the smaller the crystallite size are, the smaller *Z* values result. In fact, crystals of cotton, *Cephalocereus*, and *Pilocereus* are much smaller than those of algal and animal celluloses. In addition, Nishimura et al.¹⁷ has already pointed out that the diffraction peak position tends to shift toward a higher angle (larger *d*-spacings) in proportion to the decrease in the crystal size. Therefore we assume that the shift in *Z* values implies the transformation of triclinic into monoclinic units as well as the loss of crystalline perfection or reduction in crystallite size.

The authors thank Mr. S. Ui, Dr. R. H. Atalla, and Mr. K. Miura for the gift of samples that were used in this study. The study was partly supported by a Grant-in-Aid for Scientific Research, Ministry of Education and Culture, Japan (Grant nos. 63004413 and 03660163).

REFERENCES

1. R. H. Atalla, J. C. Gast, D. W. Sindrof, V. J. Bartuska, and G. E. Maciel, *J. Am. Chem. Soc.*, **102**, 3249 (1980).
2. W. L. Earl and D. L. VanderHart, *J. Am. Chem. Soc.*, **102**, 3251 (1980).
3. R. H. Atalla and D. L. VanderHart, *Science*, **223**, 283 (1984).
4. D. L. VanderHart and R. H. Atalla, *Macromolecules*, **17**, 1465 (1984).
5. F. Horii, A. Hirai, and R. Kitamaru, *Macromolecules*, **20**, 2117 (1987).
6. F. Horii, *Nuclear Magnetic Resonance in Agriculture*, Chapt. 10, P. E. Pfeffer and W. V. Gerasimowicz, Eds., CRC Press, Boca Raton, FL, 1989.
7. H. Chanzy, B. Henrissat, M. Vincendon, S. F. Tanner, and P. S. Belton, *Carbohydr. Res.*, **160**, 1 (1987).
8. A. Hirai, F. Horii, and R. Kitamaru, *Macromolecules*, **20**, 1440 (1987).
9. F. Horii, H. Yamamoto, R. Kitamaru, M. Tanahashi, and T. Higuchi, *Macromolecules*, **20**, 2946 (1987).
10. H. Yamamoto, F. Horii, and H. Odani, *Macromolecules*, **22**, 4130 (1989).
11. P. S. Belton, S. F. Tanner, N. Cartier, and H. Chanzy, *Macromolecules*, **22**, 1615 (1989).
12. J. Sugiyama, J. Persson, and H. Chanzy, *Macromolecules*, **24**, 2461 (1991).
13. J. Sugiyama, T. Okano, H. Yamamoto, and F. Horii, *Macromolecules*, **23**, 4168 (1990).
14. J. Sugiyama, R. Vuong, and H. Chanzy, *Macromolecules*, **24**, 4168 (1991).
15. T. Okano and A. Koyanagi, *Biopolymers*, **25**, 851 (1986).
16. E. M. Debzi, H. Chanzy, J. Sugiyama, P. Tekely, and G. Excoffier, *Macromolecules*, **24**, 6816 (1991).
17. J. Nishimura, T. Okano, and I. Asano, *Mokuzai Gakkaishi*, **27**, 709 (1981).

Received July 6, 1992

Accepted December 23, 1992